Proc. NIPR Symp. Antarct. Meteorites, **8**, 215–224, 1995

MAGMATIC REPLACEMENT PROCESSES IN UREILITES

Olga B. MITREIKINA, Nina G. ZINOVIEVA and Lev B. GRANOVSKY

Department of Petrology, Faculty of Geology, Moscow State University, Lenin Gory, Moscow 119899, Russia

Abstract: Detailed studies of ureilites (Novo-Urei, Havero, Dyalpur, Kenna) showed that this type of achondrite had formed in a similar manner to intrusive rocks intensely affected by explosive reducing metal melts rich in hydrocarbon fluids. The reverse zoning of olivine and pyroxene of the ureilite resulted from these alterations. The reverse zoned structure is accompanied by an increase of Mg content in the margins of both minerals and the formation of so-called "interstitial material", which is a product of intense recrystallization and partial melting of the olivine and pyroxene at their contacts with metal-carbon veins. The zoning of the primary minerals is controlled by the configuration of the veins. The higher the intensity of the recrystallization process, the more extensive are alterations of the initial rocks exerted by the hydrocarbon fluids, which produced the lherzolite-type pyrope-diamond assemblage.

1. Introduction

A critical review of the extensive literature on ureilites (GOODRICH, 1992; OGATA *et al.*, 1991; SCOTT *et al.*, 1992) has attracted the attention of researchers to the polystage character of ureilite formation. The equilibrium assemblage of the main rock-forming minerals, olivine (Fa=18–20) and pigeonite (Fs=18), reflects the process of magmatic differentiation at a low pressure, whereas the "interstitial material" mineral assemblage implies carbon-metal-silicate-CO/CO_2 equilibrium in a high-pressure process. This fact led TAYLOR *et al.* (1993) to the conclusion of the explosive evolution of the achondrite parent body. It is necessary to note that the "interstitial material" of ureilites and the matrix material of carbonaceous chondrites are similar in the isotopic composition of oxygen, the contents of carbon material, diamonds, and noble gases. This makes the problem of ureilite genesis intractable from the standpoint of the primitive chondrite condensation.

The similarity of these melts to carbonaceous chondrites is apparent when they are considered in the light of the magmatic origin of non-differentiated chondrite bodies (MARAKUSHEV and BEZMEN, 1983; MARAKUSHEV *et al.*, 1989). The primary separation of the chondrite melt into silicate and metal-silicate parts (MARAKUSHEV *et al.*, 1992; MITREIKINA *et al.*, 1992) is compatible with the concept of the later separation of the hydrocarbon matrix melt (rich in siderophile elements) of carbonaceous chondrites and the concentration of this melt in the cores of the parental bodies during the achondrite stage of their evolution. The existence of pyrope in the recrystallized areas—we have found pyrope in the Novo-Urei and

Havero meteorites (MITREIKINA *et al.*, 1994a, b)—and the assemblage of new-formed Mg-rich minerals, Fe-metal, Fe- and Si-carbides, Cr-Fe-sulfides, Cr-spinel, carbon material, and diamonds, led us to the conclusion that the recrystallization of ureilites occurred at a high fluid pressure, which is favorable to the recrystallization of ureilites under the effect of the explosive carbon-rich melts.

2. C-metal Veins

SEM (CamScan 4DV, in secondary and backscattered electrons) and microprobe examination of veins filled by carbon and carbon-metal material has shown that their structure reflects the sequence crystallization of high-pressure phases from the melt.

2.1. Morphology and mineral composition of veins

Veins have an irregular shape and form thin apophyses. Host rock fragments in them had been displaced, turned and completely crystallized by the moment of the vein intrusion (Fig. 1). Fractures between olivine and pyroxene grains and veins crossing these grains are filled with carbon material, Fe-Ni metal, carbides and sulphides. It is noteworthy that the percentage of the carbon material and metals in veins is different among ureilites, and the ureilites, whose veins are dominated by carbon material (Novo-Urei, Havero and Dyalpur), show more intense alteration of the silicates than ureilites poor in carbon component in the metal-rich veins (Kenna).

The carbon material consists of graphite, diamond, and hardly discernible fine-grained black disseminations along the veins. Because diamond has a higher density than graphite, it forms a higher relief during polishing and is thus clearly seen in the SEM secondary electron images.

2.2. Relationships of vein minerals

The kamacite forms small drops and beads in the graphite-rich areas. These beads are concentrated along the vein contacts and often show a complex structure: they consist of several agglomerated (dumb-bell shaped) drops of kamacite or both kamacite and daubreelite, sometimes with perryite. The kamacite is accompanied by equant diamond grains, which begin crystallizing from the vein walls so that the crystal tops are always directed toward the vein center (Fig. 2). Characteristic relationships of the vein minerals are shown in Fig. 3: diamond, kamacite, and daubreelite occur as complicated intergrowths, in which a kamacite drop is partially surrounded by a daubreelite rim, both being partially included in diamond. The diamond crystals grow from the vein boundary, have the cubic habit, and commonly range from 20 to 40 μm, sometimes >60 μm. The high porosity of the diamond crystals (Fig. 4) shows that the melt was rich in fruids during the diamond crystallization. The diamond and its intergrowths with kamacite are more euhedral than the graphite that dominates in the carbon veins. The graphite has been identified by its lower relief in comparison with diamond and by the typically layered structure (Figs. 1, 2). It should be noted that we found graphite pseudomorphs after diamond in none of the areas with coexisting diamond and graphite examined in the Novo-Urei, Dyalpur, Kenna and Havero meteorites. The graphite is more anhedral

Fig. 1.

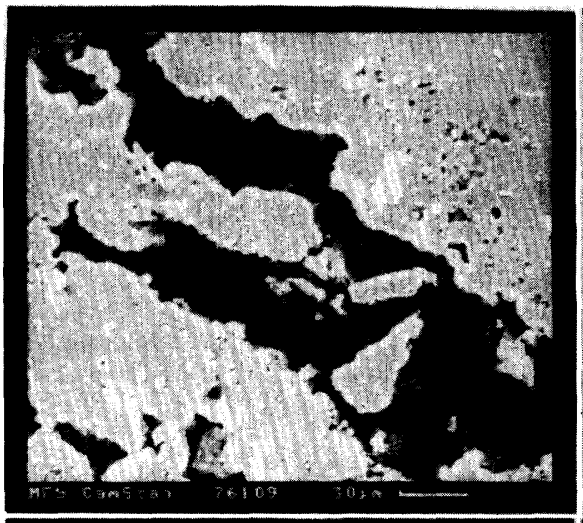

Fig. 2.

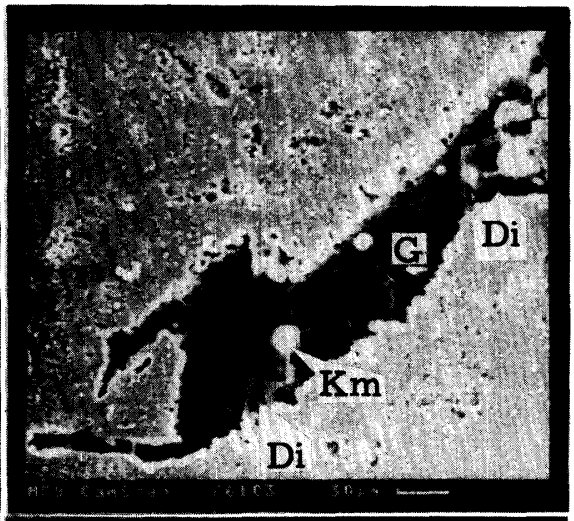

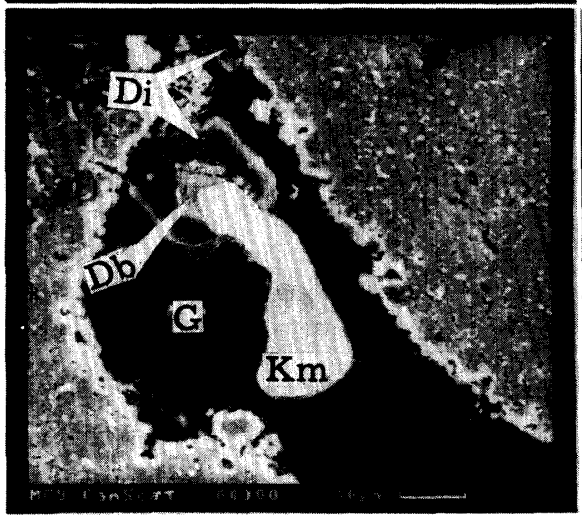

Fig. 3.

Fig. 4.

Fig. 1. Secondary electron image of a carbon-rich (graphite-dark gray) vein in the silicate (light gray) material of the Havero ureilite. Silicate fragments are turned and slightly removed.

Fig. 2. Secondary electron image of a carbon-rich vein in olivine is filled with layered-structure graphite (G) with kamacite drops (Km) and diamond crystals (Di), growing from the boundary of the vein. The Havero ureilite.

Fig. 3. Combined secondary and back-scattered electron image of an intergrowth of diamond (Di), kamacite (Km), and daubreelite (Db) in a carbon-rich vein. The Havero ureilite.

Fig. 4. Combined secondary and back-scattered electron image of a porous diamond adjacent to the boundary of a carbon-rich vein. The Novo-Urei ureilite.

than the diamond, demonstrating that the vein material crystallized with a pressure decrease.

The carbon material of metal-rich veins can be concentrated both in the vein selvages and in the central parts of the kamacite veins where the carbon material forms a fine-grained aggregate, which is hardly identifiable by SEM. The carbon material and small (up to 1–1.5 μm) carbide and silicide iron grains are evenly distributed in the kamacite veins. In places, the carbon material contains some Si and,

sometimes, Al and Ca.

Note that the distribution of the vein material is controlled by the volatility of its components. Metals are situated in the central parts of the veins, sulphides occur in the border parts, and carbon material is situated both in the central parts and around the veins in the alterated zones of silicates, which are recrystallized by hydrocarbon fluids, altering the primary composition and structure of the ureilites.

3. Recrystallization of Silicates

The alterated areas of silicates occur as thin discontinuous zonal rims along the grain boundaries or along thin veins inside the grains. The olivine grains have much thicker alteration rims than the pyroxene grains (Figs. 5a, b).

3.1. Recrystallization of olivine

The outer parts of the olivine grains (rims) are recrystallized, near the veins, into an aggregate of Mg-olivine, orthopyroxene, and Fe-metal. We found that this rim had a zonal structure (Fig. 6) with following zones, proceeding from the C-metal vein to the center of the olivine grains: (a) orthopyroxene+occasional SiO_2 grains+ carbides+carbon material+Fe-Cr sulphides+Cr-spinel; (b) orthopyroxene+olivine (Fa=2–3)+Fe-metal+carbon material+fine chromite grains; (c) olivine (Fa=5–6)+ fine Fe-metal grains+carbon material; (d) olivine (Fa=10)+fine Fe-metal grains. The Fe-content of the olivine grains increases sharply centerward and the grain centers have a constant composition (Fa=17–20) devoid of any fine intergrowths of Fe-metal. Unlike the Fe-Ni metal of the veins, the fine Fe-metal grains in the olivine never contain nickel. It should be noted that the olivine (with Fe-metal intergrowth) is deficient in ferrous iron as a result of reduction of Fe^{2+} to Fe^0 and formation of Fe-metal.

The composition of the primary olivine and the products of its recrystallization are listed in Table 1. The bulk chemistries of the completely recrystallized parts of the rim are nearly the same as those of the olivine deficient in ferrous iron. The recrystallized phases are poor in Fe, and rich in Cr. The small grains of primary olivine are completely recrystallized. The compositions of the new-formed olivine and pyroxene have a similar X_{mg}=MgO/MgO+FeO value (0.90–0.96), which is much higher than that of the primary olivine (0.69–0.75).

Thus, the zonal structure of the olivine grains has been formed due to reduction of ferrous iron and recrystallization of olivine. The discrete changes of parageneses of the recrystallized aggregate form a metasomatic zonation and show an increase of the reduction potential from the centers of the olivine grains to the fractures into which the reduced carbon-rich melt intruded.

Fine (less than 1.5 μm) grains of pyrope: Pyr-82.0, Alm-7.4, Andr-5.0, Uvar-2.3, Gros-3.3-$(Mg_{2.46}Fe^{2+}_{0.22}Ca_{0.32})(Al_{1.85}Cr_{0.04}Fe^{3+}_{0.1})[Si_{3.04}O_{12}]$ were first found (MITREIKINA *et al.*, 1994a, b) in the intensely altered olivine areas adjacent to the boundaries of C-metal veins in the Novo-Urei and Havero ureilites (Table 2). The garnet is persistently accompanied not only by orthopyroxene and almost pure forsterite but also by sporadic grains of augite and quartz. Hence, this is a typical

Fig. 5a. Fig. 5b.

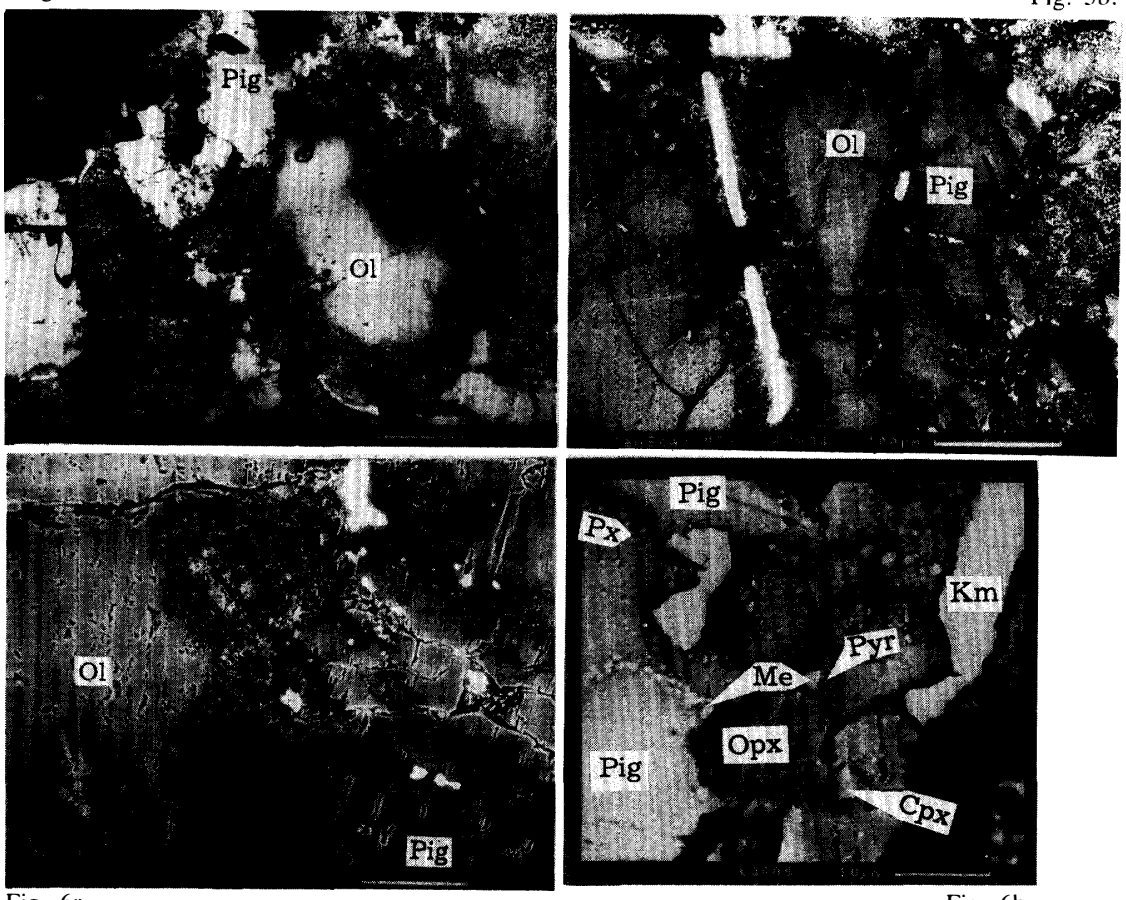

Fig. 6a. Fig. 6b.

Fig. 5. Intense alteration of olivine (Ol) and weak alteration of pigeonite (Pig) in meteorites: (a) Dyalpur, (b) Novo-Urei.

Fig. 6a. A carbon-metal vein with near-vein alteration of olivine (left) and pyroxene (right). The Novo-Urei meteorite.

Fig. 6b. Combined secondary and back-scattered electron image of a pyrope in a zone of intense alteration of pigeonite. Pyr-pyrope, Pig-pigeonite, Px-low-Ca pyroxene, Opx-orthopyroxene, Cpx-augite, Me-Fe-metal, Km-kamacite. The Novo-Urei meteorite.

pyrope-pyroxene-olivine paragenesis of lherzolite. The occurrence of this high-pressure garnet assemblage in meteorites from relatively small parent bodies confirms that the alterations occurred under high fluid pressure. The relatively small grain size and low abundance of the garnet in the intensely recrystallized areas seem to be due to moderate introduction of Al by hydrocarbon fluid into the carbon-rich veinlets.

3.2. Recrystallization of pigeonite

The pigeonite is locally recrystallized both near C-metal veins and along thin fractures cutting its grains (Fig. 5). The recrystallization zones occur as very thin and discontinuous rims and form the taxite structure of the primary pyroxene. As in the olivine, the recrystallization of the pigeonite has a zonal structure. Zone 1 (recrystallization zone)—a weak alteration of pyroxene is caused by the partial

*Table 1. Compositions (wt%) of olivine (I) and its recrystallization products (II).**

	I		II		
N	1(25)	2(18)	3(17)	4(11)	5(14)
Oxide	Ol-1	Ol-2	Ol	Opx	bulk comp.
SiO_2	39.73	40.63	41.68	57.28	41.28
Cr_2O_3	0.55	0.68	0.69	0.77	1.34
FeO	18.20	13.53	5.24	4.08	15.31
MnO	0.36	0.34	0.41	0.46	0.31
MgO	40.75	44.46	51.77	36.89	41.36
CaO	0.32	0.35	0.21	0.52	0.40
X_{mg}	0.69	0.77	0.91	0.90	0.73

*From here on we shall exemplify analyses of minerals of Novo-Urei ureilite has been carried out by SEM CamScan-4DV with energy-despersive analyzer Link An 10000. The amount of researched grains is shown in parentheses. X_{mg}=MgO/(MgO+FeO). For legend see Fig. 8.

Table 2. Phases of mineral paragenesis of the garnet-bearing zone of olivine recrystallization.

N	1	2	3	4	5	6
Oxide	Ol	Opx	Cpx	Gr1	Gr2	G1
SiO_2	42.97	57.89	52.62	47.25	45.58	63.43
TiO_2	—	—	0.36	0.36	—	—
Al_2O_3	—	—	5.37	20.28	23.73	1.56
Cr_2O_3	0.20	0.39	0.70	—	1.17	1.29
FeO	1.67	1.70	1.06	5.94	3.65	8.28
MnO	0.31	0.29	0.38	0.23	0.27	0.43
MgO	54.67	39.30	20.46	21.34	25.62	15.19
CaO	0.18	0.42	19.05	3.79	0.78	1.66
Na_2O	—	—	—	<0.2	<0.2	<0.2
K_2O	—	—	—	<0.2	0.11	
X_{mg}	0.97	0.96	0.95	0.8	0.87	

Gr1-garnet, meteorite Novo-Urei; Gr2-garnet, meteorite Havero.

Table 3. Compositions of pigeonite (I) and its recrystallization products (II).

	I		II						
N	1(12)	2(7)	3(15)	4(8)	5(7)	6(11)	7(11)	8(6)	9(5)
Oxide	Pg	Opx1	Opx2	Opx3	Cpx1	Cpx2	Gl	Q	Pl
SiO_2	55.34	57.87	58.38	59.06	56.68	56.72	74.09	93.96	69.92
TiO_2	—	—	0.18	—	0.21	0.28	—	—	0.5
Al_2O_3	0.83	—	0–0.15	—	0.76	2.48	8.21	3.40	18.12
Cr_2O_3	1.16	0.83	0.86	0.38	1.03	0.15	0.8	—	—
FeO	11.60	8.54	3.37	1.48	2.12	0.88	2.01	—	0.62
MnO	0.25	0.25	0.42	0.43	0.17	0.28	0.29	—	—
MgO	26.51	30.64	32.78	34.86	23.44	21.87	9.83	0.42	3.28
CaO	4.51	1.87	4.01	3.79	15.59	17.16	3.20	0.59	4.35
Na_2O	—	—	—	—	—	0.19	1.25	1.32	3.03
K_2O	—	—	—	—	—	—	0.23	0.4	0.17
X_{mg}	0.69	0.78	0.91	0.96	0.91	0.96			

reduction of ferrous iron and formation of fine Fe-metal grains. The altered pyroxene (Table 3, N 2) is poor in Ca and completely devoid of Al in comparison with the pigeonite core (Table 3, N 1). This low-Ca orthopyroxene forms as thin rim around pigeonite grains near the C-metal veins and as areas of weak alteration inside pigeonite grains. Ca and Al are concentrated in the central part of the altered area

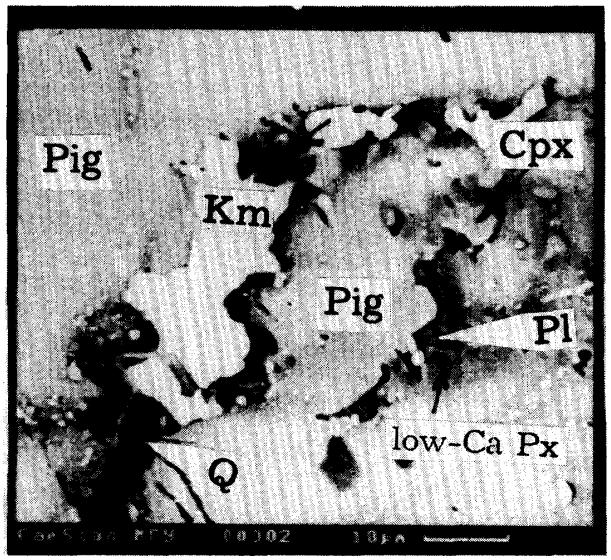

Fig. 7. A melted zone in pigeonite of the Dyalpur meteorite.

(zone 2). Zone 2 (melting zone)—the zone of active pyroxene recrystallization—consists of low-Ca pyroxene (Table 3, N 3, 4), augite, and silicate glass with a variable content of Al_2O_3 and alkalis. The newly-formed low-Ca pyroxenes have metastable composition, which is inherent in ureilites. The texture of this zone shows evidence of melting: small (up to 2–3 μm) euhedral augite grains grow on the surface of low-Ca pyroxene crystals, and these grains, together with small grains of Fe-metal, are cemented by an interstitial quatz-like phase. The bulk composition of the recrystallized areas of pigeonite is the same as the composition of the primary pigeonite (Table 3). The melting zone has a normative composition of pyroxene only in restricted "melted pockets" within the pigeonite grains. Sometimes this melt intrudes along fractures into unaltered zones of the pigeonite (Fig. 7) and even into partially recrystallized grains of olivine. The contents of SiO_2, Al_2O_3, and alkalis of the glass increase toward the "melted pockets", and both quartz and plagioclase appear in the interstices between the newly-formed pyroxene grains (Table 3, N 8, 9).

4. Discussion

Comparison of the newly-formed mineral parageneses replacing the olivine and pyroxene shows that they formed under local equilibrium conditions. The X_{mg} value (0.69–0.72) of the primary pigeonite is equal to that of the olivine cores, and the X_{mg} value (0.90–0.96) of mineral phases in the recrystallized areas of the pigeonite is equal to the X_{mg} value of the olivine recrystallization products. The increase in the X_{mg} value of the silicates is discrete, which is controlled by changes of relatively stable mineral assemblages of the recrystallized zones (Figs. 8, 9). Obviously, the attainment of local equilibrium during the recrystallization of olivine and pyroxene rules out any possibility of their impact genesis. The ureilite recrystallization is of a facial-isochemical nature and does not require any transport of major elements. The

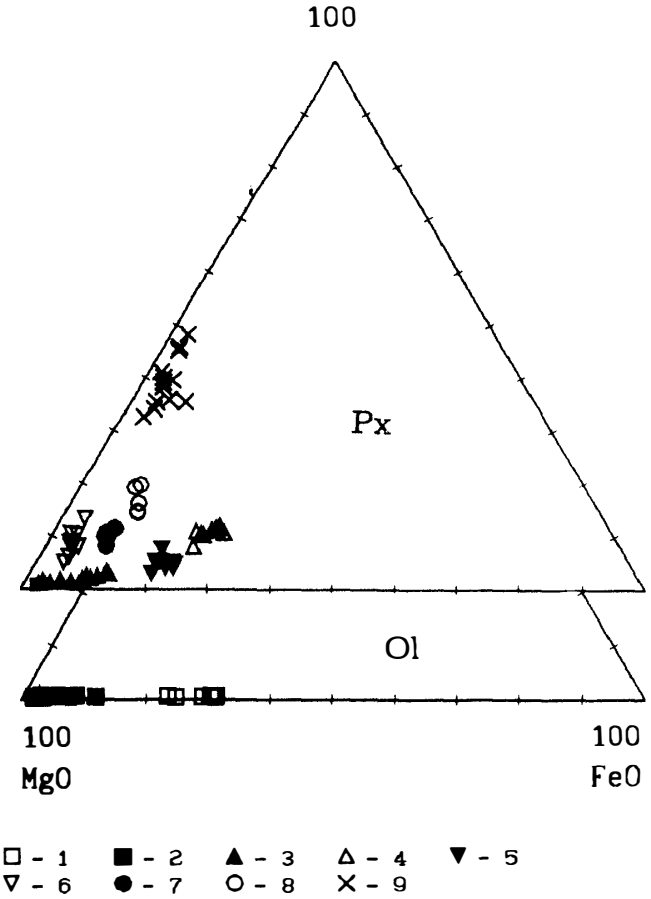

Fig. 8. A MgO-CaO-FeO diagram of olivine and pyroxene compositions of the Novo-Urei ureilite: (1–4) zone recrystallization of olivine: 1—core of the primary olivine (Table 1, N 1); 2—weakly-altered olivine (Table 1, N 2); 3—olivine of a recrystallization zone (Table 1, N 3, Table 2, N 1); 4–orthopyroxene of a recrystallization zone (Table 1, N 4, Table 2, N 2); (5–9) zone recrystallization of pigeonite: 5—primary pigeonite (Table 3, N 1); 6—weakly altered pyroxene (Table 3, N 2); 7, 8—low-Ca pyroxene (Table 3, N 3, 4); 9—augite (Table 3, N 5, 6).

interstitial material of ureilites is well known (GOODRICH, 1992; OGATA *et al.*, 1991) to have a heterogeneous distribution of Si, Ca, Al, Cr, and alkalis. As was mentioned above, this heterogeneous distribution is related to different compositions of the primary olivine and pyroxene, and thus there is no need to invoke any residual, interstitial melt of the ureilites. The morphology of C-metal veins shows that the ureilite substrate had completely crystallized by the moment when the fluid melts intruded into the veins. The discrete alterations of the ureilite primary mineral compositions are controlled by the intrusion of metal melts rich in hydrocarbon. This alteration reflects the influence of reducing fluids (gradually neutralized by the rock) on the surrounding minerals. The pressure of a hydrocarbon fluid is responsible for the active olivine recrystallization and for the pyroxene partial melting. This pressure is high enough to form the pyrope-diamond assemblage. The comparison of ureilites,

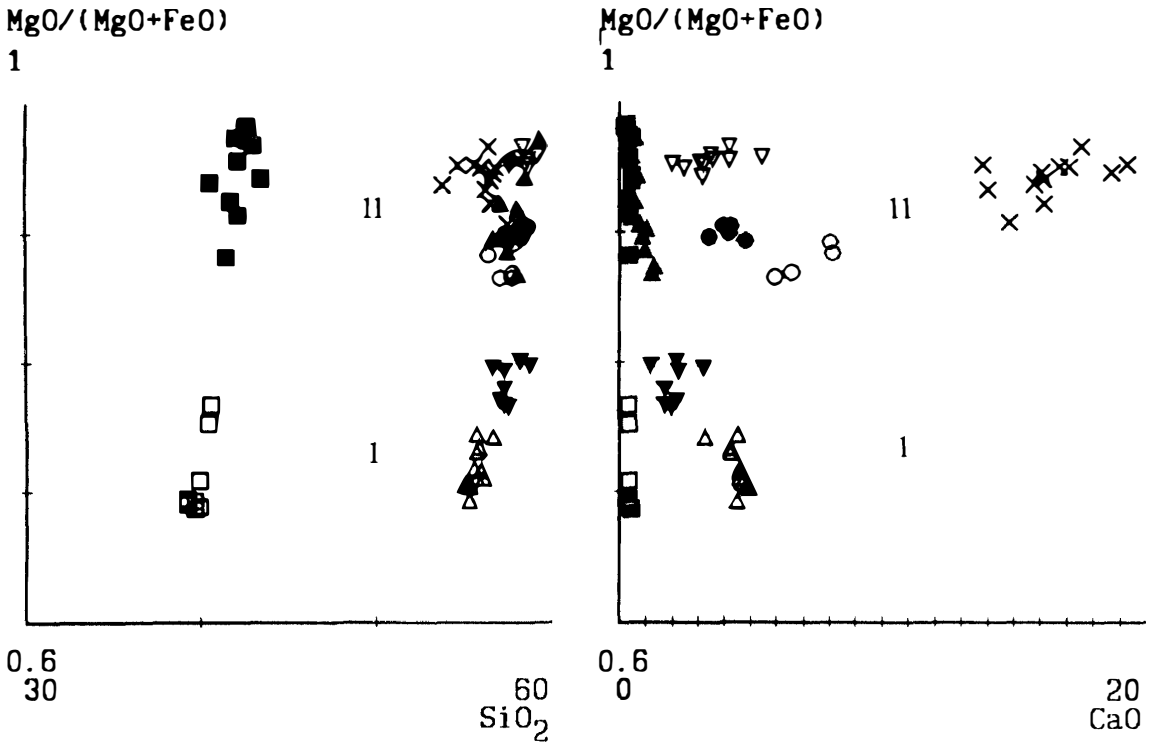

Fig. 9. Compositional discrete-gradual alteration of olivine and pyroxene of the Novo-Urei ureilite. I-weak alteration zone; II-active alteration zone. For legend see Fig. 8.

which had undergone impact metamorphism of different grade, showed that the processes of recrystallization and impact metamorphism were independent. The occurrence of glass in the melted zones of pyroxene and the small thickness of the recrystallized zones of primary ureilite material support the concept of the explosive character of this process and testify to the high neutralization rate of reducing fruids in the crystalline ureilite material.

Acknowledgments

This research described in this contribution was made possible in part by Grant N MU 8000 from the International Science Foundation and by Grant 94-05-16942 from the Russian Fund of Fundamental Researches.

References

GOODRICH, C. A. (1992): Ureilites: A critical review. Meteoritics, **27**, 327–352.

MARAKUSHEV, A. A. and BEZMEN, N. I. (1983): Evolutsiya meteoritnogo veschestva, planet i magmaticheskich serii (Evolution of meteorite substance, planets and magmatic series). Moscow, Nauka Press 184p.

MARAKUSHEV, A. A., GRANOVSKY, L. B., ZINOVIEVA, N. G. and MITREIKINA, O. B. (1989): Chondritovyi maagmatizm (Chondrite magmatism). Vestnik Moskovskogo Universiteta, Seriya Geologiya (J. Moscow Univ., Geol.), **1**, 3–19.

MARAKUSHEV, A. A., GRANOVSKY, L. B., ZINOVIEVA, N. G. and MITREIKINA, O. B. (1992): Kosmicheskaya

Petrologiya (Space Petrology). Moscow University Press, 325p.

MITREIKINA, O. B., ZINOVIEVA, N. G. and GRANOVSKY, L. B. (1992): Petrologicheskiye prisnaki likvatsionnogo mechanizma chondroobrasovania (Petrological features of the liquid immiscibility mechanism of the chondrites formation). Vestnik Moskovskogo Universiteta, Seriya Geologiya (J. Moscow Univ., Geol.), **1**, 38–48.

MITREIKINA, O. B., CHRUIKINA, O. V., ZINOVIEVA, N. G. and GRANOVSKY, L. B. (1994a): Mineral paragenesis of the ureilites: Evidence for high pressure in a large parent body. Lunar and Planetary Science XXV. Houston, Lunar and Planet. Inst., 909–910.

MITREIKINA, O. B., ZINOVIEVA, N. G. and GRANOVSKY, L. B. (1994b): Magmatic replacement processes in ureilites. Papers Presented to the 19th Symposium on Antarctic Meteorites, May 30–June 1, 1994. Tokyo, Natl Inst. Polar Res., 118–121.

OGATA, H., MORI, H. and TAKEDA, H. (1991): Mineralogy of interstitial rim materials of the Y74123 and Y790981 ureilites and their origin. Meteoritics, 26, 195-201.

SCOTT, E. R. D., KEIL, K. and TAYLOR, G. J. (1992): Origin of ureilites by partial melting and explosive volcanism on carbon-rich asteroids. Lunar and Planetary Science XXIII. Houston, Lunar Planet. Inst., 1253–1254.

TAYLOR, G. J., KEIL, K., MCCOY, T, HAACK, H. and SCOTT, E. R. D. (1993): Asteroid differentiation: Piroclastic volcanism to magma oceans. Meteoritics, **28**, 34-52.

(*Received August 15, 1994; Revised manuscript received January 20, 1995*)